Use of a Seeing Monitor to Determine the Velocities of Turbulent Atmospheric Layers

Richard Roosen

University of Minnesota, 200 Union St. S.E., Minneapolis, MN 55455

Jeffrey Meisner

Leiden Observatory, Postbus 9513, 2300 RA Leiden, The Netherlands

Abstract.

Using the illumination of an arbitrary bright star, a schlieren optical system at the focus of a .75m telescope has been successful in imaging atmospheric turbulence. Such an apparatus translates the gradient of atmospheric phase variations into intensity variations. A CCD camera captures snapshots of the resulting pattern at a 60Hz frame rate.

Successive frames are cross-correlated in order to extract the velocity vectors of winds affecting the turbulent layers responsible for astronomical seeing. The velocities of strong turbulent layers may be detected in as little as one second with the present apparatus, allowing the observation of transient atmospheric turbulent phenomena on such a time scale. Proposed enhancements would increase the sensitivity of the system to weaker features, and a system for simultaneously determining the altitude of the atmospheric layers associated with the wind velocities is suggested.

Due to its ability to identify the individual contributions of distinct atmospheric layers towards seeing, such an apparatus may have use as a realtime seeing monitor in conjunction with ground based interferometers and adaptive optics systems, as well as in statistical studies of seeing, site selection, and meteorological research.

1. Introduction

Astronomical "seeing" is caused by turbulent motion and mixing in the atmosphere involving air masses of different refractive indices (mainly due to temperature variations), and is responsible for degrading the point spread function of optical astronomical images well beyond the diffraction limit of the telescopes. An adaptive optics system attempts to detect and correct for the distortion present in a received wavefront over a large aperture. Similarly, a long-baseline interferometer performing fringe-tracking must follow the differential atmospheric delay affecting the light received at separated points. In all such ground-based astronomical observations, quantitative knowledge of the statistical characteristics of atmospheric phase variations can be employed to better adapt the instrument for, and calibrate the results of, observations made under those conditions. Specific measures of wind velocities and the heights of turbulent layers may be used to optimize the operation of more sophisticated adaptive optics systems, such as configurations involving wavefront correctors projected to the altitudes of two or more specific turbulent atmospheric layers (Shamir 1993). Additionally, seeing monitors are used for observatory site characterization and selection, and in general studies of the atmosphere and optical propagation through it, as we have performed with the apparatus to be described.

In addition to various active techniques (such as LIDAR or use of balloon borne instruments) there are numerous optical configurations which can perform remote sensing of turbulent atmospheric layers simply using the light from a bright star. Recording detailed short exposure images at the focal plane of a telescope, better known as *speckle interferometry* (Labeyrie 1970), will yield random "speckle" patterns characterized by a power spectrum determined by the telescope aperture, the luminous object, and the statistics of the atmospheric delay function. In the case of a point source such as a single star, the effect of the atmosphere will be dominant, thus providing a measurement of atmospheric turbulence parameters (Dyck 1983). One can employ a Hartmann sensor which will directly measure the wavefront tilt at each of numerous sub-apertures defined by a lenslet array or mask (Bally 1996). A shearing interferometer can similarly be used to detect wavefront variations across a large aperture (Dainty 1974). The differential atmospheric delay between isolated points can be observed directly by tracking a white-light fringe (or fringes produced from narrowband light with a phase-unwrapping algorithm) using a long-baseline interferometer (Buscher 1994), or an interferometer using short baselines produced by aperture masking on a large telescope (Haniff 1994). The effect of phase variations at high altitudes will produce intensity variations, or *scintillation* at the earth's surface which can be directly observed; intentional misfocussing of the field lens will allow low altitude phase variations to be likewise observed as if the scintillation had been observed directly from the bottom of a deep pit (Klückers, 1997). The *curvature sensor* (Roddier 1988) proposed for adaptive optics wavefront sensing is a refinement of this principle.

In the present experiment, light from a bright star is brought to a focus at which point the beam is partially obstructed by a knife edge. The then-diverging light is collected by a field lens which images the telescope aperture onto a CCD detector (Figure 1, left pane). The spatial filter thus implemented provides an image of phase variations in the wavefront due to the atmosphere (Figure 2). *Schlieren* systems of this sort are commonly used to image flow and turbulence in fluids having temperature or pressure variations. Such an optical system is also used to test the wavefront integrity of optical components, such as telescope objectives, in which case it is referred to as the *Foucault knife edge test.*

To the best of our knowledge, the first use of such an optical system on a telescope using light from a star corrupted by the atmosphere, was reported by Hartmann (1908) who noted that instantaneous images thus obtained combined refractive errors in the optics with the random effect of the atmosphere. Using a photographic time exposure to perform long-term averaging, the random atmospheric variations are removed, yielding a pattern diagnostic of the telescope optics (such as we produced by digitally averaging 500 frames, shown in the rightmost image of Figure 2). Similar subsequent use of starlit schlieren imag-

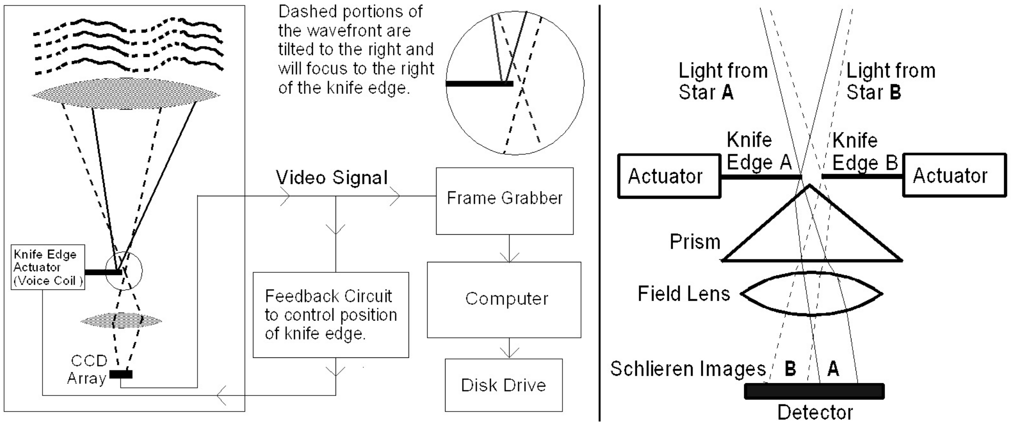

Figure 1. Left: Hardware configuration used. Right: Proposed system to record two schlieren images using a binary star (Section 4.).

ing by Horace Babcock led to his appreciation of the character of atmospheric optical effects and his proposal (Babcock 1953) for the real-time correction of such wavefront aberrations, a technique now known as *adaptive optics.*

It has long been appreciated that observation of the motion of scintillation patterns or "flying shadows," readily observed by eye at the focus of a large telescope with the eyepiece removed, would directly yield wind velocities attributable to the turbulent atmospheric layers involved. Attempts to thereby observe such velocities using dynamic scintillation patterns have been performed indirectly using high speed photometric measurements on discrete apertures (Protheroe 1961, Rocca 1973), or directly using imaging cameras and correlation by computers (Azouit 1980, Klückers 1997). Unlike the latter experiment in which use of a binary star enabled wind velocities to be measured for an identified layer of turbulence at a specific altitude, in the present work using schlieren optics, the contributions of atmospheric turbulence at all altitudes are combined with equal weight. The results can be viewed in a map of atmospheric turbulence strength versus wind vector, such as shown in Figure 4. consisting both of clear peaks (corresponding to wind velocities at particular altitudes) and continuum regions (corresponding to a range of wind velocities, presumably over a range of altitudes). Although seeing *per se* (image distortion at the focal plane) is dependent only on the unweighted contribution of all turbulent layers, knowledge of altitude may be desired not only for general atmospheric studies, but in the determination of anisoplanaticity due to the increased weight from atmospheric turbulence at higher altitudes. A proposal for the extension of our method for concomitant determination of altitude information using illumination from a binary star is briefly presented in Section 4..

2. Method and Apparatus

The optical system used consists of the University of Minnesota's .75 meter O'Brien telescope with a knife edge placed at the f/10 Cassegrain focus followed by a field lens (f=8mm) and a CCD video camera. The knife edge translates

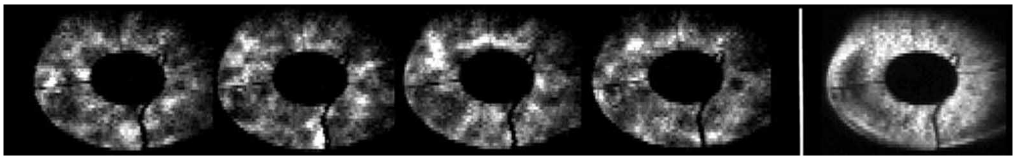

Figure 2. Four consecutive video frames of schlieren data. Rightmost image is the average of 500 frames, revealing imperfect telescope optics.

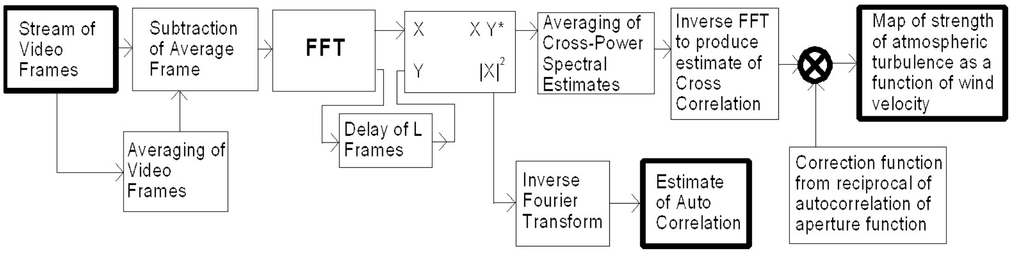

Figure 3. Processing of digitized video stream (Figure 2) from CCD.

phase variations of the wavefront to intensity variations on the CCD. The transfer function is derived in the appendix, but a geometric optics approximation may be understood as follows (Figure 1, left pane). A plane wave incident upon the telescope will focus to a point near the optic axis shifted laterally according to its tilt. The incident wavefront can be viewed as a collection of sub-apertures each with its own tilt. Since the knife edge will block the light from subapertures whose wavefronts are tilted to the left (see inset), the imaged intensity is related to the slope of the phase at each section of the wavefront.

The acquisition hardware includes a COHU model 4915-2000 CCD camera (shutter speeds of $1/500^{th}$ or $1/1000^{th}$ of a second are used to avoid smearing fast moving features), a Data Translation model DT3155 frame grabber, and a computer. A control loop detects the average image intensity and controls an actuator to keep the knife edge bisecting the star's image in the focal plane. This feedback loop insures maximum contrast and a consistent system response.

Since the CCD images features related to the phase of the wavefronts, winds driving the turbulent layers cause them to move across the field. By cross-correlating successive frames, wind velocities can be extracted. The maximum velocity which can be detected will be the telescope diameter divided by the video frame period, or in our case 45 m/sec (35 m/sec is achieved in practice).

The data reduction is diagramed in Figure 3. After removal of the average, each frame I_i is Fourier transformed: $H_i = \mathcal{F}\{I_i - \overline{I}\}$. The products of the transforms of successive frames are formed and averaged over N frames:

$$\overline{S_{xy}} = \frac{1}{N}\sum_{i=1}^{N} H_i H_{i+1}^*$$

The inverse transform, $\mathcal{F}^{-1}\{\,\overline{S_{xy}}\,\}$ will be an estimate of the cross-correlation between successive frames. Increasing N, the number of cross-correlation estimates averaged, will be at the expense of obscuring short lived phenomena.

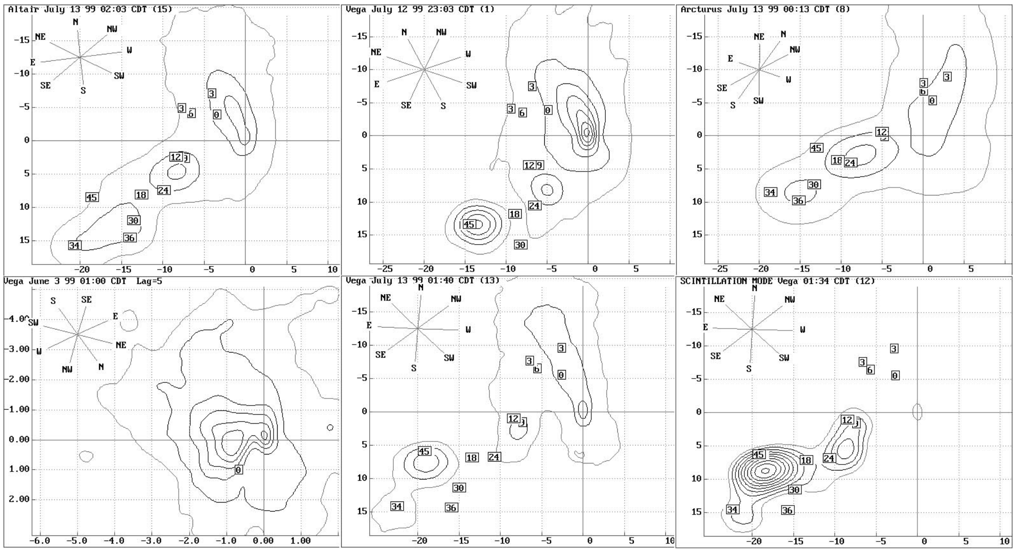

Figure 4. Correlation maps using 3 different stars (upper panes). Low velocity analysis using a lag of 5 frames (lower left). Schlieren results (lower center) are compared with correlations obtained from scintillation (lower right) data. Wind velocities are in meters/second.

While cross-correlating adjacent frames serves to reveal wind velocities up to the maximum mentioned above, correlations with frame lags L greater than one (i.e. from $< H_i H^*_{i+L} >$) are useful for determining the velocities of slower winds with greater resolution. The squared magnitude of the Fourier transforms $|H_i|^2$ are also inverse transformed to yield the autocorrelation, whose width is expected to follow changes in the Fried parameter r_o.

3. Results

Useful data (see Figure 2) were recorded on three nights using four different bright stars (Vega, Arcturus, Altair, and Capella). In each case data reduction yielded specific velocities of one to three upper air currents, and measurement of low altitude phenomena including "dome seeing."

The top three panes of Figure 4 show the results of schlieren data taken using three different stars on the night of July 12, 1999. Correlation using 1 frame lag has broken down the net strength of atmospheric seeing (i.e. $\int C_n^2\, dh$) as a function of wind velocity. Outside (light) contours are at the 2σ level; bold contours are highly significant. Available meteorological data for estimated wind speeds at various heights are projected onto the plane normal to the line of sight to the star, and are plotted on each graph with boxes containing the applicable altitudes as expressed in thousands of feet. Those points are reasonably consistent with the observed data, and the observations at three different perspectives (using different stars) are consistent with each other. Meteorological variations are also evident over the period of the observations.

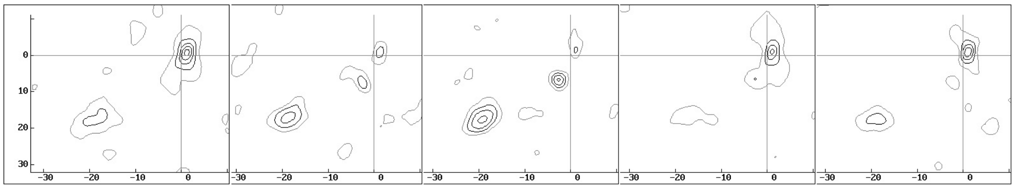

Figure 5. Velocity maps each produced from only one second of data, depict significant changes (bold contours) in 3 features over 5 seconds.

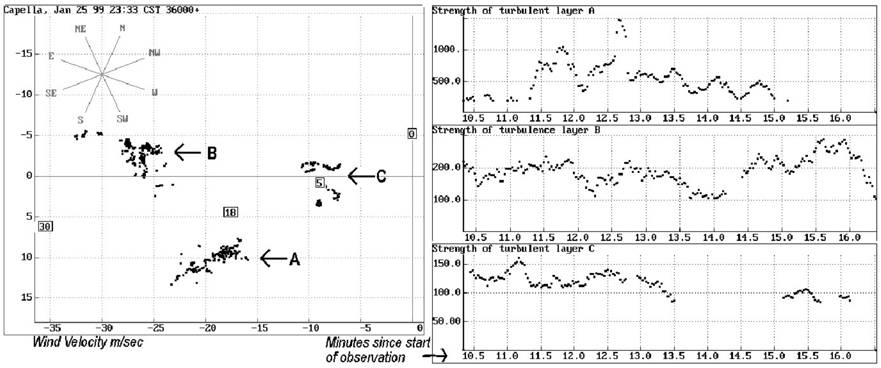

Figure 6. Left: Plot of positions of peaks for 3 upper air wind velocities tracked over a period of 6 minutes. Right: Strength of each feature (when clearly observed) is plotted over time.

In one experiment, the knife edge was removed from the optical system in order to image *scintillation* alone. Comparison of the correlation thus obtained (Figure 4, lower right) with the results of a contemporaneous schlieren observation (to its left) reveals agreement in identifying two upper air currents. As expected, however, the band of velocities apparently due to low altitude or surface winds, detected by the schlieren apparatus, is absent from the velocity map produced by the scintillation data. More detailed maps of apparent surface winds have been produced from schlieren data by correlating images using lags of more than one frame period ($1/60^{th}$ second). A correlation over 5 frame periods is shown in Figure 4, lower left.

While the results shown in Figure 4 each represent the integration of about a minute of data, we have typically found it possible to identify the peaks of correlation due to strong layers of upper air turbulence with integrations of less than 10 seconds. In Figure 5, for instance, correlations each using only one second of data (60 frames) reveal rapid changes in the presence of turbulent features at two upper air locations, and at the surface, over a 5 second interval. Examination of three correlation peaks in Figure 6 over a period of 6 minutes, reveals random changes in the contributions of each, albeit with poorer temporal resolution. The positions of the three peaks over this period are plotted on the left pane (with boxes again representing meteorological reports), and the strengths of the three peaks (in identical arbitrary units) are plotted in three graphs on the right side. In order to reliably track the features it was necessary to perform moving averages over a period of 10 seconds for the 'A' peak, 30 seconds for the weaker 'B' peak, and 50 seconds for the even weaker 'C' peak. Data are not plotted for times at which a peak was not clearly identified, or was at a level not clearly distinguishable from noise.

4. Conclusions and Future Work

The work reported herein has demonstrated, using modest equipment, the feasibility of an atmospheric seeing monitor based on a schlieren optical system using light from a bright star. In addition to its ability to detect changes in the parameters describing the magnitude and dynamics of seeing, the apparatus is distinguished by its ability to directly extract wind velocities of turbulent atmospheric layers contributing to seeing. Detection of wind velocities driving the strongest turbulent layers were clearly determined using as little as 1 second of data. It can be concluded that by employing a more powerful computer and a small telescope, one could thus implement a realtime seeing monitor to be used, perhaps, in support of a long-baseline interferometer or adaptive optics system.

In addition to not having been tested at a site of good astronomical seeing, the system that was built for this experiment was limited in a number of ways. More thorough studies of atmospheric turbulence would be aided by using a larger telescope, since a larger aperture area would proportionately reduce the observation time required to achieve a given level of sensitivity. In addition to detecting weaker turbulent features, this would allow the detection and velocity determination of shorter lived turbulent phenomena. While a high speed shutter is always required, an increased frame rate video camera would capture more images and more photons, also leading to an increase in net sensitivity. The apparatus could function using light from somewhat dimmer stars by using a faster field lens (at the expense of spatial resolution), or from *much* dimmer stars, using an image intensified camera.

Simultaneous determination of the *altitudes* of turbulent atmospheric layers at which detected winds are present, might be obtained with the proposed apparatus depicted in Figure 1, right pane. This configuration requires illumination of the turbulent atmospheric layer by a suitable binary star. The converging beams from each component of the binary will be offset at the telescope focus, where separate knife edges are controlled to bisect the light of each beam. The schlieren patterns illuminated by each star are separately imaged, resulting in atmospheric optical features being detected with a parallax proportional to the altitude of the turbulent layer responsible. One would be able to observe altitudes up to $h_{max} = D/\phi$ where D is the aperture diameter and ϕ is the angular separation between the stars. Alternatively, a coarse determination of altitude might be obtained simply by a comparison of the strengths of correlations from simultaneously obtained schlieren and scintillation data (as in Figure 4).

References

Shamir, J., Crowe, D. G., Beletic, J. W. 1993, Appl.Optics, 32, 4618

Labeyrie, A. 1970, A&A, 6, 85

Dyck, H. M., Howell, R. R., 1983, PASP, 95, 786

Bally, J., Theil, D., Billawala, Y., Potter, D., Loewenstein, R. F., Mrozek, F., Lloyd, J. P. 1996, Publ. Astron. Soc. Australia, 13, 22

Dainty, J. C., Scaddan, R. J. 1974, MNRAS, 167, 69

Buscher, D. F. 1994, Proc. SPIE, 2200, 260

Haniff, C., Baldwin, J. E., Warner, P. J., Scott, T. R. 1994, Proc. SPIE, 2200, 407

Klückers, V. A., Wooder, N. J., Nicholls, T. W., Adcock, M. J., Munro, I., Dainty, J. C., 1997, A&AS, 130, 141

Roddier, F. 1988, Appl.Optics, 27, 1223

Hartmann, J. 1908, ApJ, 27, 254

Babcock, H. W. 1953, PASP, 65, 229

Protheroe, W. M. 1961, Science, 134, 1598

Rocca, A., Roddier, F., Vernin, J. 1974, JOSA, 64, 1000

Azouit, M, Vernin, J. 1980, J. Atmos. Sci., 37, 1550

5. Appendix: Optical System Response Function

Since a knife edge is placed at the focus (Fourier plane), it acts as a spatial filter and (neglecting scale factors) the electric field at the image plane E_2, will be the inverted incident field E_1, convolved with the Fourier transform of the transmittance function of the knife edge.

$E_2(x,y) = E_1(-x,-y) \bigotimes \mathcal{F}\{t_f\}$

The knife edge can be represented by $t_f(x,y) = \frac{1}{2}[1 + sgn(x)]$

Its Fourier transform is:

$\mathcal{F}\{t_f\} = \frac{1}{2}[\delta(x) - \frac{1}{j\pi x}]\delta(y)$

Thus we have:

$E_2(x,y) = \frac{E_1(-x,-y)}{2} + \frac{j}{2\pi}\int_{-\infty}^{\infty} d\xi \frac{E_1(-\xi,-y)}{x-\xi} = \frac{1}{2}[E_1(-x,-y) + \frac{j}{\pi}\int_{-\infty}^{\infty} ds \frac{E_1(s-x,-y)}{s}]$

We recognize the integral to be the Hilbert transform in x of $E_1(-x,-y)$.

Let us now consider the special case of a phase only function whose phase varies linearly with x in a region of size Δs around $-x$:

$E_1(-x+s,-y) \approx E_o\, e^{j\gamma s} \quad \text{for } |s| < \frac{\Delta s}{2}$

Due to the $1/s$ term in the integration kernel, we may be able to crudely approximate the integral by only integrating over the region $-\frac{\Delta s}{2} < s < \frac{\Delta s}{2}$:

$\int_{-\infty}^{\infty} ds \frac{E_1(s-x,-y)}{s} \approx \int_{-\frac{\Delta s}{2}}^{\frac{\Delta s}{2}} ds\, E_o\, e^{j\gamma s} = j\, E_o \int_{-\frac{\Delta s}{2}}^{\frac{\Delta s}{2}} ds\, \frac{sin(\gamma s)}{s} \approx j\, E_o\, \Delta s\, \gamma$

The final approximation requires $\Delta s\, \gamma \ll 2\pi$, so as to keep the region of the integration well within the main lobe of the sinc function. Finding the intensity:

$I_2(x,y) = |E_2(x,y)|^2 \approx \frac{1}{4}|E_o|^2(1 - \frac{2\,\Delta s}{\pi}\gamma + \frac{\Delta s^2}{\pi^2}\gamma^2)$

Thus we have the original intensity modulated by first and second order terms. Note that the first order term is linearly dependent on γ, the slope of the phase. Since, for an achromatic wavefront tilt, γ is inversely proportional to wavelength, we find that the contrast varies as $1/\lambda$.